Desalination and Water Treatment
www.deswater.com
doi: 10.1080/19443994.2015.1098567

57 (2016) 19333–19343
September

Taylor & Francis
Taylor & Francis Group

Increased removal of Reactive Blue 72 and 13 acidic textile dyes by *Penicillium ochrochloron* fungus isolated from acidic mine drainage

Pınar Aytar[a,*], Damla Bozkurt[a], Seda Erol[b], Mine Özdemir[b], Ahmet Çabuk[a,c]

[a]*Department of Biotechnology and Biosafety, Graduate School of Natural and Applied Sciences, Eskisehir Osmangazi University, 26480 Eskisehir, Turkey, Tel. +90 222 239 37 50, ext. 2757; Fax: +90 222 239 35 78; emails: pinaraytar@gmail.com (P. Aytar), ddamlabozkurt@gmail.com (D. Bozkurt), ahmetcabuk@gmail.com (A. Çabuk)*
[b]*Department of Chemical Engineering, Eskisehir Osmangazi University, 26480 Eskisehir, Turkey, emails: serol@ogu.edu.tr (S. Erol), mnozdemi@ogu.edu.tr (M. Özdemir)*
[c]*Faculty of Arts and Science, Department of Biology, Eskisehir Osmangazi University, 26480 Eskisehir, Turkey*

Received 12 September 2014; Accepted 16 September 2015

ABSTRACT

In this study, acidic textile dyes, including Reactive Blue 13 and Reactive Blue 72, were adsorbed by *Penicillium ochrochloron* AMDB-12 isolated from acidic mine drainage. Optimal conditions in terms of pH, initial dye concentration, agitation rate, biomass dosage, contact time, and temperature for this process were determined. Biosorption yields for RB13 and RB72 were 55 and 61%, respectively, under determined optimum conditions. These conditions were determined to be a contact time of 120 min, pH 2, an agitation speed of 150 rpm, and an initial dye concentration of 50 ppm for both dyes, while biosorbent dosages were 1 and 2 g L^{-1} for RB72 and RB13, respectively. The biosorption of all dyes was endothermic in nature. The biosorbent was characterized using Fourier transform infrared spectroscopy, scanning electron microscopy, and energy-dispersive X-ray spectroscopy before and after dye biosorption. The Langmuir model was found most suitable for describing the biosorption of all dyestuffs. The experimental data fit very well with the pseudo-second-order kinetic model.

Keywords: Biosorption; Acidic textile dyes; *Penicillium ochrochloron*

1. Introduction

The use of synthetic dyes has been rising in many fields, including textile, pharmaceutical, pulp and paper, paint, plastics, and cosmetics industries [1]. The wastewaters of these dyestuffs lead to serious environmental problems, which have produced large concerns over the effects of synthetic dyes on the environment. These dyestuffs have been found to inhibit photosynthetic events. Furthermore, the rigid environmental regulations relating to discharge of these effluents have increased researchers' concerns over efficient treatment methods. Therefore, the decolorization of industrial textile effluents is a significant environmental problem [2,3]. Several physicochemical methods, such as ozonation, oxidation, ion exchange, irradiation, chemical coagulation/flocculation precipitation, and adsorption, are used for dye decolorization [4]. Although these methods are practicable, they are costly, inefficient, and have operational problems [5]. Biological methods, including microbial decolorization, have

*Corresponding author.

been increasingly utilized in dye wastewaters over recent decades. In general, microbial biomass is a practical option for the treatment of textile industry effluents [6–8].

It is known that widely available biosorbents have been used for dye removal. These microorganisms, such as bacteria, fungi, algae, and yeasts, efficiently adsorb a vast range of dyes [7,9]. Among these microorganisms, fungi have been increasingly utilized for biosorption in recent years. Fungal biomass obtained from inexpensive medium and facile fermentation techniques are easily applicable to industrial fermentation processes [10,11].

Acid mine drainage (AMD) has a low pH, high concentration of heavy metals, and high specific conductivity, and it harbors both prokaryotes and eukaryotes, including fungi such as *Aspergillus* sp., *Talaromyces* sp., *Penicillium* sp., and *Bispora* sp., which are known to play an important role in microbial mat and streamer formation [12,13]. These organisms have significant potential for use in biotechnological applications, including decolorization of acidic textile dye wastewater [14–16].

Penicillium is one of the most extensive fungi in the terrestrial environment. *Penicillium* has been utilized for dye removal via biodegradation/biosorption [17–19]. *Penicillium restrictum* had been recently used for biosorption of Reactive Black 5 [17]. Yang and coworkers studied *Penicillium* YW 01 for biosorption capacities of Acid Black 72 and Congo Red under different conditions [20]. According to the study of Shedbalkar et al., when biodegradation of Cotton Blue by *Penicillium ochrochloron* MTCC517 was studied, the bacterial (using *A. vinelandii*) toxicity test showed a growth inhibition zone around the well-containing Cotton Blue [18]. The same researchers found that Malachite Green was effectively degraded at pH 7 by *P. ochrochloron*, although fungi prefer acidic pHs [21].

P. ochrochloron AMDB-12 was isolated from an AMD (Turkey) in our previous study, rather than terrestrial source. The isolation of fungi from extreme environments, such as AMD, is significant for understanding not only biodiversity but also alternative metabolic pathways for biotechnological application. The correlation between fungus isolation source and biotechnological application, including acidic textile dye adsorption, encouraged the utilization of this fungus in the current study. For this purpose, biosorption of selected acidic textile dyes was carried out using the obtained fungal biomass. Relationships between the dye decolorization process and physicochemical parameters were characterized to achieve maximum dye removal. Finally, analyses of Fourier transform infrared spectroscopy and Scanning electron microscopy (SEM) before and after the biosorption process were performed. In addition to thermodynamic parameters, the data were evaluated using kinetic and isothermal models.

2. Materials and methods

2.1. Dyestuffs and chemicals

Reactive Blue 13 (RB13) (λ_{max} 568 nm) and Reactive Blue 72 (RB72) (λ_{max} 627 nm) are commonly used dyes in the textile industry. They were obtained from a textile industry in Turkey. In this study, maximum absorbance peak wavelengths of RB13 and RB72 were determined prior to use.

2.2. Microorganism growth conditions

AMD water samples were collected in 2012 from Balya AMD (Balikesir province, Turkey) for isolation of the fungus. Metal mining has been continued in this field since that time. The pH value and amount of dissolved oxygen for this drainage were 3.05 and 5.15 mg L^{-1}, respectively. Fungal isolation was performed using these water samples. AMD samples (20 mL) were filtered through a 0.45 μm membrane. Filters were placed onto media containers with malt extract agar (pH 2.5) or dichloran 18% glycerol agar. The plates were incubated for 7 d at 25°C. The fungal isolate was further subcultured using malt extract agar.

The fungus was identified as *P. ochrochloron* AMDB-12 with GenBank accession number KF588636 in our previous study. This fungal isolate was grown on malt broth slants for 7 d at 25°C to prepare the mycelium suspension. Then, a mycelium suspension (1 mL) of *P. ochrochloron* AMDB-12 was added to malt broth under aseptic conditions. The flasks were incubated at 30°C with shaking at 150 rpm for 7 d. The fungal cells were then filtered and dried in an oven at 60°C. The dried biomass was ground and sieved to select particle sizes of less than 300 μm and stored for use.

2.3. Optimization studies

Batch biosorption studies were conducted using dyestuff solutions in 250 mL Erlenmeyer flasks with a 50 mL working volume. Concentrated dye solutions were prepared as stock solution and then 50 mL of dye solutions were used for experiments prepared from dilution of concentrated solutions. Samples were shaken at given appropriate time and then centrifugated at 10,000 rpm for 5 min. The supernatants were used for analysis. The flasks were exposed to various biosorbent dosages, pH values, initial dyestuff concentrations, agitation rates, temperatures, and contact

times to determine the optimum biosorption conditions. All experiments were performed in triplicate.

Batch biosorption parameters were tested for initial pH (1.0–7.0), biosorbent dosage (0.1–3 g L^{-1}), contact time (10–360 min), initial dye concentration (10–200 mg L^{-1}), and agitation rate (50–200 rpm). The pH of the solution was adjusted with NaOH or HCl.

2.4. Theoretical basis

The amount of dye adsorbed by fungus biomass was calculated from the differences between the dye amount added to the biomass and the dye amount after the biosorption experiment using the following equation:

$$q_e = \frac{(c_0 - c_e)v}{m} \quad (1)$$

To determine the kinetics of the biosorption process, experimental data were evaluated using two kinetic models (Eqs. (2) and (3)): Lagergren pseudo-first-order and pseudo-second-order equations [22]. The pseudo-first-order equation is given as:

$$\log(q_e - q_t) = \log q_e - \frac{k_1 t}{2,303} \quad (2)$$

where k_1 (min^{-1}) is the pseudo-first-order rate constant, q_e and q_t are the amount of dye adsorbed (mg g^{-1}) at time t and at equilibrium, respectively.

The pseudo-second-order equation may be expressed in the form:

$$\frac{t}{q_t} = \frac{1}{k_2 q_e^2} + \frac{t}{q_e} \quad (3)$$

where k_2 (g mg^{-1} min^{-1}) is the pseudo-second-order rate constant of pseudo-second-order biosorption [23].

The analysis of equilibrium data is important for the development of mathematical models that could be used to investigate the biosorption mechanism. Langmuir, Freundlich, and Dubinin–Radushkevich (D–R) isotherm models are used to describe the biosorption isotherm [24]. Linear forms of these equations are given using the following formulas (Eqs. (4) and (5) [25,26]:

$$\frac{C_e}{q_e} = \frac{1}{bq_0} + \frac{C_e}{q_0} \quad (4)$$

$$\log q_e = \log K_f + \frac{1}{n}\log C_e \quad (5)$$

$$\ln q_e = \ln q_m - \beta\varepsilon^2 \quad (6)$$

where q_e is the amount of adsorbed dye per amount of biosorbent at equilibrium (mg g^{-1}), C_e is the equilibrium concentration in the solution (mg L^{-1}), and the Langmuir constants, q_0 (mg g^{-1}) and b (L mg^{-1}), are the monolayer adsorption capacity and the adsorption equilibrium constants, respectively. The monolayer adsorption capacity and equilibrium constant of biosorption, K_f and n, respectively, are Freundlich coefficients associated with the adsorption capacity and intensity, respectively. q_m is the D–R adsorption capacity (mg g^{-1}), β is the constant associated with adsorption energy (mol^2 kJ^{-2}), and ε is the Polanyi potential.

The Polanyi potential is given as:

$$\varepsilon = RT \ln(1 + (1/C_e)) \quad (7)$$

where R is the gas constant (kJ mol^{-1} K^{-1}) and T is the temperature (K).

The mean energy of adsorption (E) is calculated using the following equation:

$$E = (2\beta)^{-0.5} \quad (8)$$

$$R_L = \frac{1}{1 + bC_0} \quad (9)$$

where C_0 is the initial dye concentration (mg L^{-1}). The values of R_L calculated from the above equation are incorporated (Eq. (9)).

The thermodynamic parameters, change in free energy (ΔG°), enthalpy (ΔH°), and entropy (ΔS°), for the adsorption process were calculated using the Langmuir equilibrium constants (b). These parameters are calculated from the following formulas (Eqs. (10) and (11)):

$$\ln b = \frac{\Delta S^\circ}{R} - \frac{\Delta H^\circ}{R}\left(\frac{1}{T}\right) \quad (10)$$

$$\Delta G^\circ = \Delta H^\circ - T\Delta S^\circ \quad (11)$$

where R is the gas constant (8.314 J mol^{-1}) and T is the solution temperature (K). The values of ΔH° and ΔS° are calculated from the slope and intercepts, respectively, of the equation of the plotted data. Using these values, ΔG° can be calculated.

2.5. FTIR and SEM analyses

FTIR spectra of unloaded and dye-loaded biosorbents were recorded on a Bruker Tensor 27 infrared spectrometer in the region of 400–4,000 cm^{-1} for determining the types of functional groups on the biosorbent surface. SEM was carried out to determine potential changes in the biosorbent particle surfaces using a JEOL 5600 LV SEM instrument.

3. Results and discussion

3.1. Optimization studies

The effect of pH on the biosorption process was investigated by varying pH values from 1.0 to 7.0, and the results are presented in Fig. 1(a). Because of the fact that degradative effect of lower pH on dye degradation, we used control experiment at whole initial pH tests without biomass. The obtained % biosorption values during the ph optimization in this experiment were investigated with these control tests. In this study, the optimum pH was found to be 2.0 for each dye (28% biosorption for RB13 and 38% for RB72). This finding is because the biosorption value of *P. ochrochloron* AMDB-12 at strong acidic pH values increases from 1.0 to 2.0. As shown in the literature, a high biosorption yield was observed under these acidic conditions [27,28]. The pH of the aqueous solution can change the biosorbent charge value and thereby affect the adsorption of the altered groups. According to the study by Palmieri et al., the adsorption of acidic dye was optimum at acidic pH due to an increase in the protonation of weak base groups of bound biomass [29].

The effects of biosorbent dosage on RB13 and RB72 biosorption were studied at 30˚C with pH 2 and an agitation rate of 150 rpm. The dosage was varied from 0.1 to 3.0 g L^{-1}, as shown in Fig. 1(b). These results showed that biosorbent dosages were optimal at 2 and 1 g L^{-1} for RB13 and RB72, respectively. The biosorption yield increased with increasing biosorbent dosage, which provides the dyestuff molecules with more surface area for attachment [30].

Erlenmeyer flasks containing dye solutions at 50 mg L^{-1} were placed on a shaker at varied revolutions per minute (0, 50, 100, 150, and 200 rpm). Samples were kept at 30˚C for 60 min. As indicated in Fig. 1(c), 150 rpm was selected for further experiments because the decolorization percentage did not significantly increase above 150 rpm. The increase of % biosorption with increasing agitation rates up to 150 rpm was attributed to an increased mass transfer rate [31].

The impact of contact time on dye biosorption was investigated by utilizing different contact periods at three different temperatures (20, 30, and 40˚C). As indicated in Fig. 2, the adsorption capacity increased with increasing contact time up to 120 min, at which point the maximum dye adsorption capacity was reached. After 120 min, there were no further increases in the biosorption capacity; therefore, 120 min was determined to be the equilibrium contact time. This result may be due to all the biosorbent sites being empty at the initial time, resulting in a higher dye concentration gradient. After equilibrium, the biosorption profile over time for both dyes reached a plateau, suggesting that a monolayer coating of dye may have been obtained on the *P. ochrochloron* AMDB-12 surface at that point. It has been reported that the majority of biosorption occurs at early contact times due to abundantly available active sites, and the process slows with the passage of time due to electrostatic repulsion between adsorbed and unadsorbed dye molecules [32]. Similar results were found in the literature [33]. Thus, the dye adsorption rate by the *P. ochrochloron* AMDB-12 biomass decreased due to the decreased number of biosorption sites and the dye concentration gradient [34]. It can also be observed from Fig. 2 that the adsorption capacity of the *P. ochrochloron* AMDB-12 biomass was enhanced with an increase in temperature from 20 to 40˚C. This result indicated that the adsorption process was endothermic, which is further demonstrated by the results in Section 3.4.

3.2. Kinetic parameters

Kinetic models of dye and metal biosorption are available in the literature [35,36]. The estimation of the biosorption rate via modeling provides data to help design adsorption systems. To determine the kinetics of dye uptake, optimum operational conditions were used in this study, as shown in Fig. 3. The biosorption equilibrium was nearly established in 120 min for both dyes at 20, 30, and 40˚C, and it was nearly constant when the biosorption capacities for RB13 were 12.30, 13.13, and 14.17 mg g^{-1} at 20, 30 and 40˚C, respectively, and when the biosorption capacities for RB72 were 23.40, 27.10, and 31.50 mg g^{-1} at 20, 30, and 40˚C, respectively (Fig. 2). The pseudo-first-order and pseudo-second-order models were tested to identify the adsorption kinetics.

The plots of $(q_e - q_t)$ vs. t, t/q_t vs. $t^{1/2}$ used for these models were checked graphically. The parameters of biosorption kinetics were calculated using linear least-squares fittings as shown in Table 1.

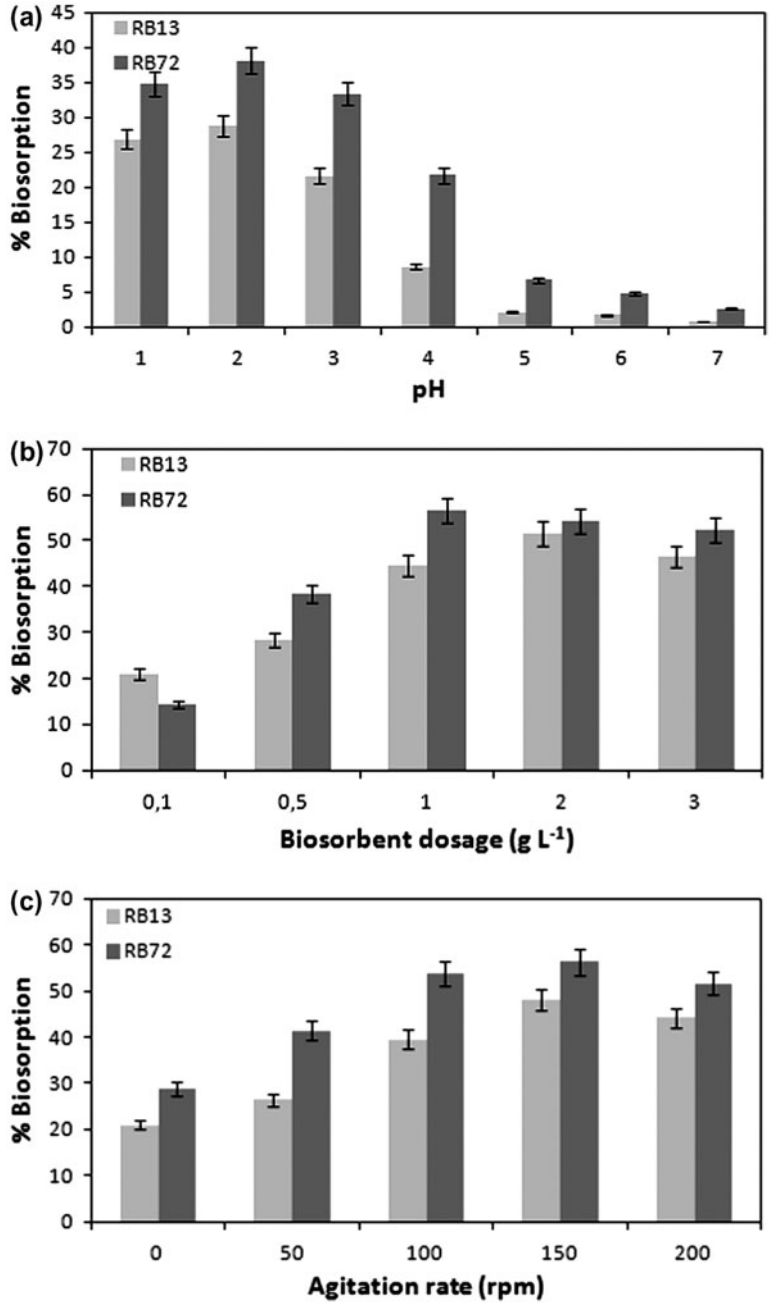

Fig. 1. Effects of selected parameters on % biosorption. (a) Effect of pH, (b) Effect of biosorbent dosage, and (c) Effect of agitation rate.

The pseudo-second-order kinetic model was found to correlate well with the experimental data. The kinetic parameters of these models were calculated, as shown in Table 1. The pseudo-second-order kinetic model was in better agreement with the experimental data than the pseudo-first-order kinetic model. Correlation coefficients of the pseudo-second-order kinetic model were higher, and the calculated q_e values agreed very well with the experimental data. The q_{max} values estimated from the pseudo-second-order kinetic model were also in good accordance with the experimental data ($q_{eq,exp}$ values at all dye concentrations of RB13 and RB72). These results demonstrate that the boundary layer resistance was not the rate-limiting step because the dye-biosorption follows pseudo-second-order kinetics [37].

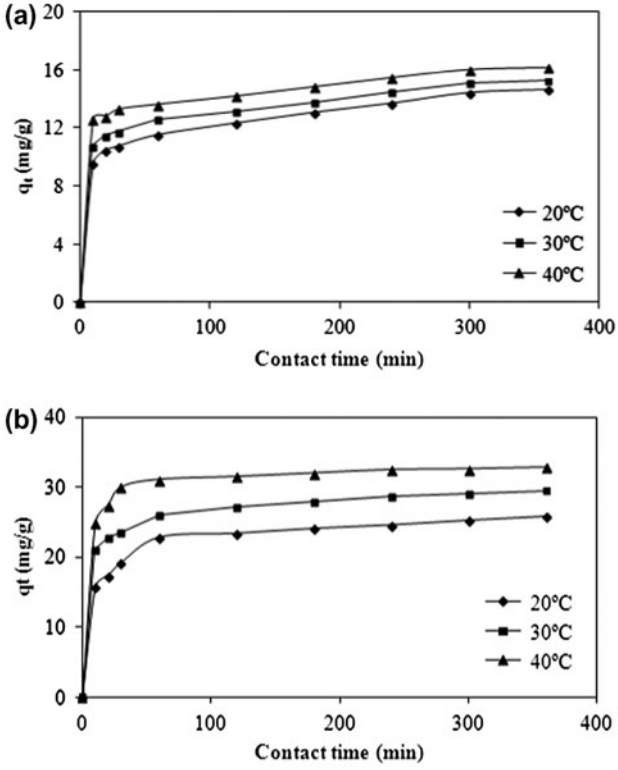

Fig. 2. Effect of contact on the biosorption of (a) RB13 and (b) RB72 by *P. ochrochloron* at different temperatures (pH 2.0; biosorbent dosage: 2 and 1 g L^{-1}, respectively; agitation rate: 150 rpm; initial dye concentration: 50 mg L^{-1}).

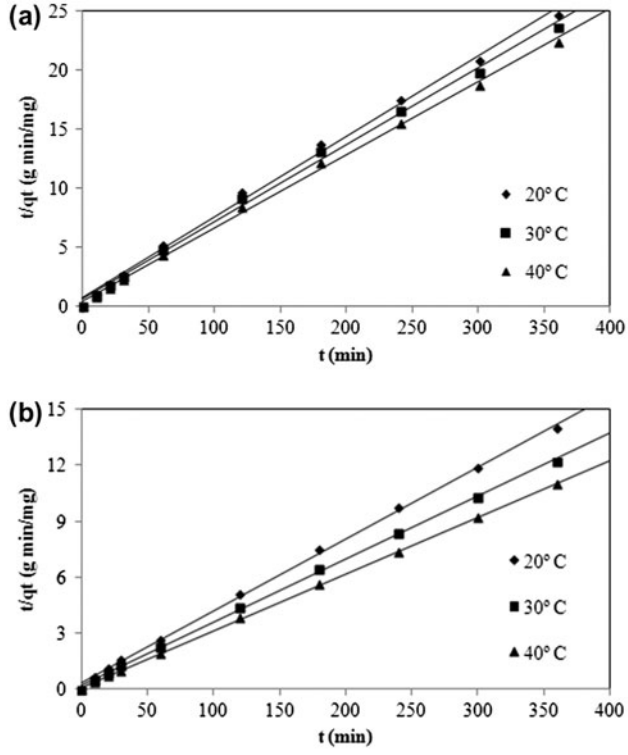

Fig. 3. Pseudo-second-order kinetic plots for the biosorption of (a) RB13 and (b) RB72 onto *P. ochrochloron* at different temperatures.

3.3. Isotherm experiments

The biosorption performance of *P. ochrochloron* biomass on RB72 and RB13 was investigated by the biosorption equilibrium measurements at different initial concentrations. The relationship between the amount of adsorbed dyes and equilibrium concentration in the solution was described by the Langmuir, Freundlich, and D–R isotherms. The biosorption data from five variable initial concentrations, 10, 20, 30, 40, and 50 mg L^{-1}, were analyzed at pH 2.0 for 120 min and temperatures of 20, 30, and 40°C. The adsorption capacity of the biosorbent increased with initial concentration and temperature. When the initial dye solution concentration was increased from 10 to 50 mg L^{-1}, the adsorption capacities increased from 4.18 to 12.31 mg g^{-1} at 20°C and from 4.28 to 14.16 mg g^{-1} at 40°C for RB13, and they increased from 9.05 to 23.45 mg g^{-1} at 20°C and from 10.15 to 31.15 mg g^{-1} at 40°C for RB72.

The linear correlation coefficients and isotherm constants are given in Table 2. The Langmuir isotherm model was more suitable for both dyes, as demonstrated by higher R^2 values compared with those of the Freundlich isotherm model. The Langmuir isotherm is specific for monolayer biosorption. The values of equilibrium coefficient, *b*; increased with an increasing of temperature.

As the R_L values lie between 0 and 1, the adsorption process is favorable [29]. Furthermore, the R_L values for dye biosorption at 40°C are between 0.014 and 0.079 for RB13 and between 0.020 and 0.090 for RB72. The maximum adsorption capacities were determined to be 14.57 and 32.25 mg g^{-1} at 40°C for RB13 and RB72, respectively, as indicated in Table 2.

The D–R isotherm was also used to estimate the biosorption characteristics of RB13 and RB72 by *P. ochrochloron* AMDB-12. The E values were 2.24–2.67 kJ mol^{-1} and 1.00–2.89 kJ mol^{-1} for RB13 and RB72, respectively (Table 2). These low *E* values demonstrated that the biosorption has a physical nature. The linear regression values (R^2) indicate that the experimental data fit well to the D–R isotherm model.

3.4. Thermodynamic parameters

Thermodynamic parameters were studied to better understand the effects of temperature and to determine

Table 1
Kinetic parameters for the biosorption of RB13 and RB72 on *P.ochrochloron* biosorbent

		Pseudo-first-order			Pseudo-second-order		
T (℃)	q_{exp} (mg g^{-1})	q_e (mg g^{-1})	k_1 (min^{-1})	R^2	q_e (mg g^{-1})	k_2 (g mg^{-1} min^{-1})	R^2
RB13							
20	14.600	5.802	9.21×10^{-3}	0.911	14.663	6.18×10^{-3}	0.995
30	15.266	5.434	9.90×10^{-3}	0.885	15.314	7.11×10^{-3}	0.997
40	16.133	4.560	9.44×10^{-3}	0.881	16.155	8.38×10^{-3}	0.998
RB72							
20	25.800	8.379	8.98×10^{-3}	0.939	25.907	4.64×10^{-3}	0.999
30	29.491	7.793	9.21×10^{-3}	0.974	29.240	6.22×10^{-3}	0.999
40	32.825	5.638	11.75×10^{-3}	0.913	32.787	10.44×10^{-3}	0.999

Table 2
Isotherms used for the description of dyes adsorption on *P.ochrochloron* cells and calculated adsorption (K_f, q_o, q_m,b, n, R_L, β, E) and correlation (R^2) coefficients

	Langmuir					Freundlich			Dubinin–Radushkevich (D–R)			
T (℃)	q_{exp} (mg g^{-1})	q_0 (mg g^{-1})	b (L mg^{-1})	R^2	$R_{L(10–50)}$	K_f (L g^{-1})	n	R^2	q_m (mg g^{-1})	β (mol^{-2} kJ^{-2})	R^2	E (kJ mol^{-1})
RB13												
20	12.31	12.64	1.06	0.999	0.086–0.019	17.47	2.07	0.699	11.54	0.1	0.977	2.24
30	13.14	13.51	1.11	0.999	0.083–0.018	19.21	2.03	0.631	12.72	0.1	0.998	2.24
40	14.16	14.58	1.32	0.999	0.071–0.015	22.71	1.81	0.691	13.12	0.06	0.969	2.89
RB72												
20	23.45	24.94	0.52	0.997	0.162–0.037	32.29	2.18	0.691	22.34	0.5	0.985	1.00
30	27.05	28.17	0.70	0.996	0.126–0.028	41.88	1.87	0.849	23.06	0.09	0.875	2.34
40	31.15	32.26	0.97	0.996	0.094–0.020	57.52	1.62	0.784	26.34	0.06	0.895	1.89

the feasibility of the adsorption process. The values of ΔH° and ΔS° were calculated from the slopes and intercepts of the linear regression of ln b vs. $1/T$. The ΔG° values were then calculated using Eq. (7). Negative ΔG° values demonstrated that the biosorption of RB13 and RB72 by *P. ochrochloron* fungus is a feasible and spontaneous process for the studied temperature range (Table 3). Furthermore, the degree of spontaneity increased with increasing temperature. Positive ΔH° values demonstrated that the adsorption is an endothermic process. Positive ΔS° values indicated an increase in the degree of freedom at the solid/solution interface and reflected the affinity of the biosorbent toward the dye molecules.

3.5. Biosorption characterization

The selected fungus for these biosorption experiments was identified in our previous study as *P. ochrochloron* AMDB-12 with GenBank accession number KF588636. Similar to our work, *P. ochrochloron* has been isolated from an acidic environment and utilized for the bioleaching of metals and for investigating mold resistance by other researchers; therefore, it is known to exhibit tolerance to harsh conditions [38]. This organism was found to be able to grow in an electroplating bath with copper levels in excess of 5 g L^{-1} [39]. Thus, this resistant fungus has been investigated for a variety of biotechnological applications. Crusberg proposed the potential ability of this fungus to precipitate different heavy metals, such as copper, lead, nickel, and cadmium [40]. Furthermore, mycelial pellet formation within 48 h by *P. ochrochloron* upon exposure to pyrene was previously found [41].

To confirm the existence of functional biosorption groups (i.e. amino, carboxyl, and phosphate) on the fungal biomass, FTIR spectra of fungal biomass preparations were obtained. The band positions of the main functional active groups are presented in Table 4. Alterations in the peaks of biomolecules associated with adsorption were considered to reflect biosorption.

Table 3
Thermodynamic parameters for the biosorption of RB13 and RB72 on *P. ochrochloron* biosorbent

	T (°C)	ΔG° (kJ mol^{-1})	ΔH° (J mol^{-1})	ΔS° (J mol^{-1} K^{-1})
RB13	20	−41.845	8.254	142.843
	30	−43.273		
	40	−44.702		
RB72	20	−56.367	23.933	192.460
	30	−58.292		
	40	−60.216		

The broad absorption peaks at approximately 3,433, 3,377, and 3,394 cm^{-1} indicate the presence of carboxylic acid or amino groups for unloaded, RB13-loaded, and RB72-loaded biosorbents. Symmetrical and asymmetrical absorption bands of –CH stretching can be seen in the range of 2,977–2,362 cm^{-1} for both unloaded and dye-loaded biosorbents. However, an adsorption band that corresponds to –COOH stretching at 2,515 cm^{-1} was observed for unloaded biomass and was absent in spectra of dyestuff-loaded biomasses. The bands observed at 3,433–2,856 cm^{-1} might reflect –CH aliphatic and aromatic groups. Amide-I peaks are visible at 1,647 and 1,651 cm^{-1} for RB13 and RB72, respectively, but they were not observed in unloaded biosorbent spectra. There is –C–C═C asymmetric stretching in both dye-loaded biomasses, with none observed in the unloaded biosorbent. The peak at approximately 1,240 cm^{-1}, not shown in the unloaded biomass spectra, is attributed to –SO_3 stretching for both loaded biomasses. The symmetrical and asymmetrical bands of –CH shifted from 2,977 to 2,925 cm^{-1} for unloaded and dye-loaded biomasses, respectively. Characteristic absorption peaks for phosphate groups at approximately 1,078 cm^{-1} for RB72 and 1,080 cm^{-1} for RB13 represent P–OH stretching, but this band was absent in the unloaded biosorbent spectra. The spectrum of each dye-loaded biomass also displayed an intensity increase in the absorption peaks at 1,380 (RB13) and 1,379 cm^{-1} (RB72), corresponding to –CH bending vibrations. –C–O stretching at 1,026 cm^{-1} for the unloaded biosorbent shifted to 1,031 and 1,029 cm^{-1} for RB13 and RB72-loaded biosorbents, respectively. Aromatic vibrations were observed at 875–709, 671–528, and 570–403 cm^{-1} for unloaded, RB13-loaded, and RB72-loaded biosorbents, respectively.

FTIR spectra of the unloaded and loaded biomasses showed that functional groups, including amide, –SO_3, hydroxyl and carboxyl groups, may be responsible for the biosorption of RB13 and RB72 onto the biosorbent. These results indicate possible involvement of the functional groups on the biosorbent surface in the biosorption process. The functional groups detected in the virgin biosorbent are likely involved in the biosorption of the evaluated dyestuffs [42,43].

It can be seen in the SEM image in Fig. 4 that the surface of the fungus biomass was heterogeneous, smooth, and porous. SEM images of the unloaded,

Table 4
Band positions before and after biosorption of reactive dyes by FTIR technique

Suggested assignment	Unloaded biomass	RB13 loaded biomass	RB72 loaded biomass
–OH and/or –NH stretching	3,433	3,375	3,394
–CH symmetric stretching	2,977	2,925	2,925
–C–H stretching	2,817	2,856	2,856
–COOH stretching	2,515	–	–
–CH asymmetric stretching	2,362	2,362	2,362
–C=O stretching vibrations	1,797	1,745	1,743
Amid-I band	–	1,647	1,651
–C–C=C asymmetric stretching	–	1,458	1,458
–OH bending vibrations	1,419	1,413	1,413
–CH bending vibrations	–	1,380	1,379
–SO_3 stretching	–	1,240	1,240
–S=O stretching	1,153	1,153	1,155
–P–OH stretching	–	1,080	1,078
–C–O stretching	1,026	1,031	1,029
–C–H bending vibrations (aromatic)	875–709	671–528	570–403

(a)

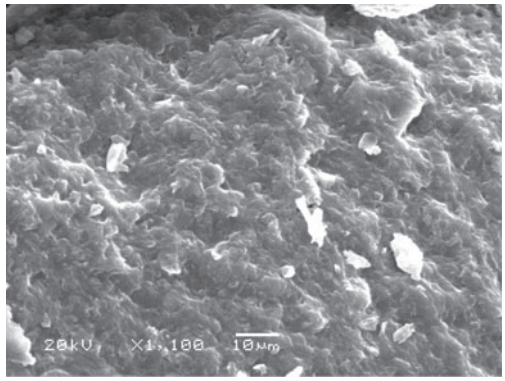

Component	Mole Conc.	Conc.
C	53.244	45.407
O	36.313	41.251
Na	0.459	0.749
Mg	0.135	0.233
K	0.952	2.643
S	0.255	0.580
Cl	0.198	0.499
Al	0.029	0.056
Ca	0.024	0.067
N	8.344	8.298
Cu	0.048	0.217
	100.000	100.000

(b)

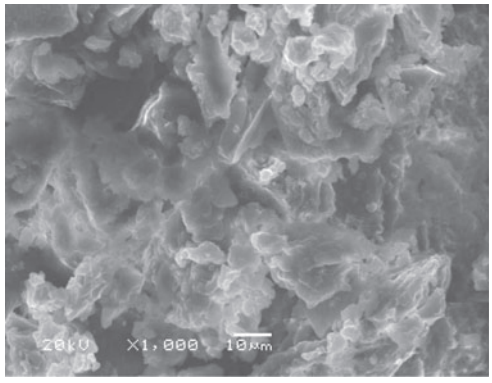

Component	Mole Conc.	Conc.
C	65.273	57.524
O	32.189	37.789
Na	0.233	0.392
Mg	0.061	0.108
K	0.521	1.496
S	0.274	0.646
Cl	0.109	0.284
Al	0.044	0.088
Ca	0.027	0.081
N	1.188	1.221
Cu	0.080	0.372
	100.000	100.000

(c)

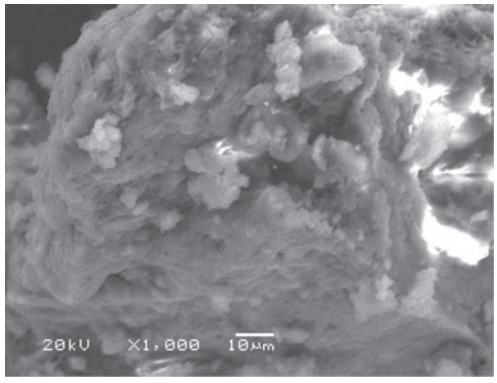

Component	Mole Conc.	Conc.
C	59.243	43.522
O	22.432	21.953
Na	0.075	0.105
Mg	0.081	0.120
K	5.523	13.209
S	0.425	0.833
Cl	5.928	12.855
Al	0.297	0.490
Ca	0.161	0.394
N	5.334	4.570
Cu	0.502	1.950
	100.000	100.000

Fig. 4. SEM micrographs and EDX analyses of natural (a) RB13-loaded biomass and (b) RB72-loaded biomass.

RB13 dye-loaded, and RB72 dye-loaded biosorbents are shown in Fig. 4(a), (b), and (c), respectively. The irregular surface provides a large surface area to the adsorbent, which in turn influences the adsorbent capacity. The change in the morphology of the dye-laden adsorbent observed in Figs. 4(b) and (c) compared with that of *P. ochrochloron* AMDB-12 in Fig. 4(a) demonstrates that the dye is adsorbed onto the adsorbent surface.

To confirm the adsorption of RB13 and RB72 onto the unloaded biomass, EDX analysis was performed, as shown in Fig. 4. The changes observed in the EDX analysis of unloaded and dye-loaded biomasses may be evidence of the responsibility of hydroxyl and carboxyl groups on the biosorbent for RB13 and RB72 biosorption [44]. This EDX result is in agreement with the FTIR data obtained in this study. Because copper is in the center of the RB72 structure, Cu amounts increased more for RB72-loaded biosorbents than for RB13-loaded biosorbents (Fig. 4(c)). According to the EDX analysis, the chloride content increased to 12.050% for RB72-loaded biosorbents, while chloride contents were 0.499 and 0.284% for unloaded and RB13-loaded biosorbents, respectively. This difference may be due to binding between the chlorides of the dye molecule and functional sites on the biosorbent. Ionic exchange and electrostatic attraction may play important roles in dye biosorption onto fungal biomass.

4. Conclusions

A fungus isolated from AMD was used in this study as a biosorbent for acidic dye adsorption. Under optimal conditions, the % dye biosorption values for RB13 and RB72 were 55 and 61%, respectively. The maximum adsorption capacities were determined as 14.57 and 32.25 mg g^{-1} at 40˚C for RB13 and RB72, respectively. Kinetic studies of this endothermic and monolayer process indicated that the pseudo-second-order kinetic model can be applied to the biosorption of RB13 and RB72. The dye-biosorbent interactions were confirmed by FTIR and EDX, and heterogeneous and porous structures were observed by SEM. Although there were studies relating to metal–biomass interaction or dye degradation in the literature, dye biosorption by a *P. ochrochloron*, an AMD isolate in this study was the first report. These results suggested that the biomass of *P. ochrochloron* AMDB-12, an isolate from Balya AMD, may be a promising low-cost adsorbent for the removal of reactive textile dyes from effluent. Further studies are considered for investigation of the removal of other textile dyes and heavy metals using *P. ochrochloron* isolate, thereby raising adsorption yield.

Acknowledgments

The authors would like to thank Dr Okan Zafer Yeşilel from the Department of Chemistry at Eskisehir Osmangazi University for the FTIR spectra of the biomass. In addition, we express our thanks to Prof. Dr Semra İlhan and Ercin Kocabiyik for identifying the fungus.

References

[1] P. Nigam, G. Armour, I.M. Banat, D. Singh, R. Marchant, Physical removal of textile dyes from effluents and solid-state fermentation of dye-adsorbed agricultural residues, Bioresour. Technol. 72 (2000) 219–226.
[2] M. Stylidi, D.I. Kondarides, X.E. Verykios, Pathways of solar light-induced photocatalytic degradation of azo dyes in aqueous TiO_2 suspensions, Appl. Catal., B Environ. 40 (2003) 271–286.
[3] M. Solís, A. Solís, H.I. Pérez, N. Manjarrez, M. Flores, Microbial decolouration of azo dyes: A review, Process Biochem. 47 (2012) 1723–1748.
[4] L. Ayed, S. Achour, A. Bakhrouf, Application of the mixture design to decolourise effluent textile wastewater using continuous stirred bed reactor, Water SA. 37 (2011) 21–26.
[5] G. Dönmez, Bioaccumulation of the reactive textile dyes by *Candida tropicalis* growing in molasses medium, Enzyme Microb. Technol. 30 (2002) 363–366.
[6] Y. Fu, T. Viraraghavan, Fungal decolorization of dye wastewaters: A review, Bioresour. Technol. 79 (2001) 251–262.
[7] A. Srinivasan, T. Viraraghavan, Decolorization of dye wastewaters by biosorbents: A review, J. Environ. Manage. 91 (2010) 1915–1929.
[8] S. Şaşmaz, S. Gedikli, P. Aytar, G. Güngörmedi, A. Çabuk, E. Hür, A. Ünal, N. Kolankaya, Decolorization potential of some reactive dyes with crude laccase and laccase-mediated system, Appl. Biochem. Biotechnol. 163 (2011) 346–361.
[9] S. Ertugrul, M. Bakır, G. Dönmez, Treatment of dye-rich wastewater by an immobilized thermophilic cyanobacterial strain: *Phormidium* sp., Ecol. Eng. 32 (2008) 244–248.
[10] A. Kapoor, T. Virarghavan, in: D. Wase (Ed.), Fungi as biosorbents, Biosorbents for Metal Ions, CRC Press, London, 1997.
[11] N. Kuyucak, B. Volesky (Ed.), Feasibility of biosorbents application, in: B. Volesky (Ed.), Biosorption of Heavy Metals. CRC Press, Boca Raton, FL, 1990.
[12] A. Akcil, S. Koldas, Acid Mine Drainage (AMD): Causes, treatment and case studies, J. Cleaner Prod. 14 (2006) 1139–1145.
[13] B.J. Baker, J.F. Banfield, Microbial communities in acid mine drainage, FEMS Microbiol. Ecol. 44 (2003) 139–152.
[14] C.I. Pearce, J.R. Lloyd, J.T. Guthrie, The removal of colour from textile wastewater using whole bacterial cells: A review, Dyes Pigm. 58 (2003) 179–196.
[15] E.S. Bireller, P. Aytar, S. Gedikli, A. Cabuk, Removal of some reactive dyes by untreated and pretreated *Saccharomyces cerevisiae*, alcohol fermentation waste, J. Sci. Ind. Res. 71 (2012) 632–639.
[16] A. Çabuk, P. Aytar, S. Gedikli, Y.K. Özel, E. Kocabiyik, Biosorption of acidic textile dyestuffs from aqueous solution by *Paecilomyces* sp. isolated from acidic mine drainage, Environ. Sci. Pollut. Res. 20 (2013) 4540–4550.
[17] C.F. Iscen, I. Kiran, S. Ilhan, Biosorption of Reactive Black 5 dye by *Penicillium restrictum*: The kinetic study, J. Hazard. Mater. 143 (2007) 335–340.
[18] U. Shedbalkar, R. Dhanve, J. Jadhav, Biodegradation of triphenylmethane dye cotton blue by *Penicillium ochrochloron* MTCC 517, J. Hazard. Mater. 157 (2008) 472–479.
[19] M. Gou, Y. Qu, J. Zhou, F. Ma, L. Tan, Azo dye decolorization by a new fungal isolate, *Penicillium* sp. QQ and fungal-bacterial cocultures, J. Hazard. Mater. 170 (2009) 314–319.
[20] Y. Yang, G. Wang, B. Wang, Z. Li, X. Jia, Q. Zhou, Y. Zhao, Biosorption of Acid Black 172 and Congo Red from aqueous solution by nonviable *Penicillium* YW 01: Kinetic study, equilibrium isotherm and artificial neural network modeling, Bioresour. Technol. 102 (2011) 828–834.
[21] U. Shedbalkar, J. Jadhav, Detoxification of malachite green and textile industrial effluent by *Penicillium ochrochloron*, Biotechnol. Bioprocess Eng. 16 (2011) 196–204.
[22] S. Lagergren, Zur theorie der sogenannten adsorption geloster stoffe (About the theory of so-called adsorption of soluble substances), Kungliga Svenska Vetenskaps akademiens, Handlingar 24 (1898) 1–39.

[23] Y.S. Ho, G. McKay, Sorption of dye from aqueous solution by peat, Chem. Eng. J. 70 (1998) 115–124.
[24] Y.G. González Bermúdez, I.L. Rodríguez Rico, E. Guibal, M. Calero de Hoces, M.A. Martín-Lara, Biosorption of hexavalent chromium from aqueous solution by *Sargassum muticum* brown alga. Application of statistical design for process optimization, Chem. Eng. J. 183 (2012) 68–76.
[25] H. Freundlich, Kolloidchemie, Akademischer Verlags geselschaft, Leipzig, 1909.
[26] I. Langmuir, The adsorption of gases on plane surfaces of glass, mica and platinum, J. Am. Chem. Soc. 40 (1918) 1361–1403.
[27] A.S. Tunalı, T. Akar, A. Çabuk, Decolorization of a Textile Dye, Reactive red 198 (RR198), by *Aspergillus parasiticus* fungal biosorbent, Braz. J. Chem. Eng. 26 (2009) 399–405.
[28] Q. Zhou, W. Gong, C. Xie, D. Yang, X. Ling, X. Yuan, Removal of Neutral Red from aqueous solution by adsorption on spent cottonseed hull substrate, J. Hazard. Mater. 185 (2011) 502–506.
[29] G. Palmieri, G. Cennamo, G. Sannia, Remazol Brilliant Blue R decolourisation by the fungus *Pleurotus ostreatus* and its oxidative enzymatic system, Enzyme Microb. Technol. 36 (2005) 17–24.
[30] G. Crını, H.N. Peındy, F. Gımbert, C. Robert, Removal of C.I. Basic Green 4 (Malachite Green) from aqueous solutions by adsorption using cyclodextrin based adsorbent: Kinetic and equilibrium studies, Sep. Purif. Technol. 53 (2007) 97–110.
[31] C. Lu, C. Liu, F. Su, Sorption kinetics, thermodynamics and competition of Ni^{2+} from aqueous solutions onto surface oxidized carbon nanotubes, Desalination 249 (2009) 18–23.
[32] L.G. da Silva, R. Ruggiero, P.M. Gontijo, R.B. Pinto, B. Royer, E.C. Lima, T.H.M. Fernandes, T. Calvete, Adsorption of Brilliant Red 2BE dye from water solutions by a chemically modified sugarcane bagasse lignin, Chem. Eng. J. 168 (2011) 620–628.
[33] M.M. Areco, L. Saleh-Medina, M.A. Trinelli, J.L. Marco-Brown, M.S. dos Santos Afonso, Adsorption of Cu(II), Zn(II), Cd(II) and Pb(II) by dead Avena fatua biomass and the effect of these metals on their growth, Colloids Surf., B Biointerfaces 110 (2013) 305–312.
[34] İ. Kıpçak, M. Özdemir, Removal of boron from aqueous solution using calcined magnesite tailing, Chem. Eng. J. 189–190 (2012) 68–74.
[35] J. Wang, C. Chen, Biosorption of heavy metals by *Saccharomyces cerevisiae*: A review, Biotechnol. Adv. 24 (2006) 427–451.
[36] T. Akar, İ. Tosun, Z. Kaynak, E. Kavas, G. Incirkus, S.T. Akar, Assessment of the biosorption characteristics of a macro-fungus for the decolorization of Acid Red 44 (AR44) dye, J. Hazard. Mater. 171 (2009) 865–871.
[37] X.J. Xiong, X.J. Meng, T.L. Zheng, Biosorption of C.I. Direct Blue 199 from aqueous solution by nonviable *Aspergillus niger*, J. Hazard. Mater. 175 (2010) 241–246.
[38] S.K. Mandal, A. Roy, P.C., Banerjee, Iron leaching from china clay by fungal strains, Trans. Ind. Inst. Met. 55 (2002) 1–7.
[39] P.M. Stokes, J.E. Lindsay, Copper tolerance and accumulation in *Penicillium ochrocloron* isolated from copper-plating solution, Mycologia 71 (1979) 796–806.
[40] T.C. Crusberg, Biomineralization of Heavy Metals within Fungal mycelia. A New Technologyfor Bioremediation of Hazardous Wastes, U.S. EPA STAR Grant R823341, (1998). Available from: <http://es.epa.gov/ncer_abstracts/grants/95/engineering/engcrusb.html>.
[41] A. Saraswathy, R. Hallberg, Mycelial pellet formation by *Penicillium ochrochloron* species due to exposure to pyrene, Microbiol. Res. 160 (2005) 375–383.
[42] R. Dolphen, N. Sakkayawong, P. Thiravetyan, W. Nakbanpote, Adsorption of Reactive Red 141 from wastewater onto modified chitin, J. Hazard. Mater. 145 (2007) 250–255.
[43] A. Saeed, M. Iqbal, S. Zafar Iqbal, Immobilization of *Trichoderma viride* for enhanced methylene blue biosorption: Batch and column studies, J. Hazard. Mater. 168 (2009) 406–415.
[44] R. Kumar, M.A. Barakat, Decolourization of hazardous brilliant green from aqueous solution using binary oxidized cactus fruit peel, Chem. Eng. J. 226 (2013) 377–383.